# Granular Co/Ag multilayers: Relation between nanostructure, and magnetic and transport properties

E. A. M. van Alphen and W. J. M. de Jonge
*Department of Physics, Eindhoven University of Technology, P.O. Box 513, 5600 MB Eindhoven, The Netherlands*
(Received 13 October 1994)

The relation between structural properties, magnetization, and magnetoresistance of sputtered Co/Ag multilayers is studied in as-deposited and annealed multilayers with thin Co layers. Nuclear-magnetic-resonance experiments and magnetization measurements showed that decreasing the nominal Co thickness below 10 Å causes a gradual transition from an anisotropic ferromagnetic layered system to a granular system consisting of a layered array of Co pancakes. Annealing extends the granular regime to larger Co thicknesses, reduces the roughness, and transforms the Co clusters to a more isotropic shape. The effect of these structural changes on magnetization and magnetoresistance is discussed.

## I. INTRODUCTION

The magnetoresistance (MR) of the Co-Ag system has been widely studied. Co/Ag multilayers have been measured with the current in the film plane[1–3] and were the first systems studied in the so called CPP (current perpendicular to the plane) geometry.[4] MR has been investigated not only in layered samples of Co and Ag but also in Co-Ag granular alloys.[5–7]

Recently there has been a great deal of interest in the influence of annealing of multilayers consisting of a stacking of very thin ($t<10$ Å) ferromagnetic layers (e.g., NiFe) and layers of an immiscible nonmagnetic element like Ag.[8–11] The purpose of the annealing treatment is to form discontinuous magnetic layers which have low saturation fields and large MR sensitivity (change in MR divided by change in applied field). Very low saturation fields ($\sim$20 Oe) are due to a soft magnetic material like NiFe, together with the applied magnetic field in the easy direction of the pancake-shaped magnetic clusters.[8,12,13]

The first part of this paper focuses on the relation between the microstructural characteristics of the Co and the magnetic and magnetotransport properties of the as-deposited Co/Ag multilayers. We will concentrate on samples which are in the transition region between multilayers and granular systems and demonstrate that these layered granular systems are formed when Co/Ag multilayers are made with very thin ($<10$ Å) Co layers. The microstructural characteristics of the Co-Ag samples were studied with $^{59}$Co nuclear magnetic resonance (NMR). This study provided information about the structure of the Co, the interface roughness, the strain of the Co lattice, and an estimation of the Co cluster size in the discontinuous Co layers.

In the second part of this paper we will study the effect of annealing of the Co/Ag multilayers on the microstructure, as obtained from NMR spectroscopy, and the consequences for magnetization and magnetoresistance. The influence of the initial microstructure on the changes in the MR upon annealing will be discussed.

## II. EXPERIMENT

Four series of Co/Ag multilayers were studied. All the samples were prepared by magnetron sputtering on Si substrates at room temperature. For all series the top and base layer were 50 Å Ag whereas the number of repetitions was kept to 100. Two series were made with deposition rates of 4 Å/s for Co and 8 Å/s for Ag. One series had a variable Co thickness ($x$ Co+20 Å Ag) and one had a variable Ag thickness (20 Å Co+$x$ Ag). The two other series were made with smaller deposition rates: 2 Å/s for Co and 4 Å/s for Ag. Again one series with a variable Co thickness ($x$ Co+20 Å Ag) and one with variable Ag thickness (6 Å Co+$x$ Ag) were made. X-ray diffractometry on the first two series confirmed the superlattice modulations and showed [111] texture. The width of the rocking curves (full width at half maximum) was about 6°.

NMR experiments were performed with a coherent spin-echo spectrometer at a temperature of 1.5 K. Magnetic fields, larger than the saturation field, were applied parallel to the film plane. During the experiments the applied field was swept at various fixed frequencies between 130 and 200 MHz. The hyperfine field $B_{hf}$ was obtained from the resonance field $B_r$ and the frequency $f$ using the relation $2\pi f=\gamma(B_{hf}-B_r)$, where $\gamma$ is the $^{59}$Co nuclear gyromagnetic ratio ($\gamma/2\pi=10.054$ MHz/T). The transverse magnetoresistance was measured at various temperatures in fields up to 1.3 T using the standard four-probe method. Successive annealing treatments were performed for 15 min in a $H_2$-$N_2$ atmosphere. Magnetization measurements were done at room temperature with a vibrating-sample magnetometer in fields up to 1.6 T and with a superconducting quantum interference device (SQUID) magnetometer at various temperatures in fields up to 5 T.

## III. AS-DEPOSITED MULTILAYERS

### A. Structure

Before we show the results of the magnetization and MR measurements on the Co/Ag multilayers we will first

0163-1829/95/51(13)/8182(11)/$06.00  

discuss the structure of the Co in these multilayers. Figure 1 shows the bulk part (Co atoms with only Co nearest neighbors) of the $^{59}$Co NMR spectrum of the 100×(40 Å Co+20 Å Ag) multilayer. The line shape of this part of the spectrum is a typical example for all the Co/Ag multilayers. For easy comparison the figure also contains the spectrum of a 1000 Å Co film in which the different contributions of fcc Co, hcp Co, and two stacking faults (sf's) between fcc and hcp Co can clearly be distinguished.[14,15] For the Co/Ag multilayer these contributions cannot be separated, but the position of the maximum and the width of the line indicate that the Co in the Co/Ag multilayers is a mixture of fcc Co, hcp Co, and stacking faults. This indication is supported by the observation that both the magnetic anisotropy and the anisotropy of the hyperfine field of the Co/Ag multilayers are between those of fcc Co and hcp Co. The large amount of stacking faults in these Co/Ag multilayers is probably produced by the partial dislocations[16] which accommodate part of the lattice mismatch between Co and Ag.[17]

We will now turn to the overall NMR spectra and their dependence on the nominal thickness of the Co layer in the range from 4 to 15 Å. In Fig. 2 these NMR spectra are plotted. The integral of the intensity is normalized to the nominal Co thickness. Apart from the intensity which arises from bulk Co nuclei around 21 T, a clear contribution at lower fields can also be observed. This intensity originates from Co atoms at the interfaces with the Ag layers. As will be substantiated in Sec. IV A, the maximum at 17.5 T can be identified with Co atoms at locally flat (111) interfaces (Co atoms with three Ag neighbors). The remaining interface intensity arises from Co atoms at imperfect surroundings, e.g., atoms at steps at the interface with 1, 2, 4, or more Ag neighbors.

Figure 3 gives a survey of the different contributions to the spectrum as a function of the nominal Co thickness. The intensities are obtained by dividing the spectra of Fig. 2 into two parts and integration of these parts (interface part 15–19.5 T, bulk part 19.5–23 T). To start with, the presence of the bulk Co signal for the sample with a nominal Co thickness of 4 Å, 2 monolayers (ML), is worth noting. This signal implicates straightforwardly that the Co did not grow in the layer-by-layer mode but presumably in three-dimensional islands, because in the

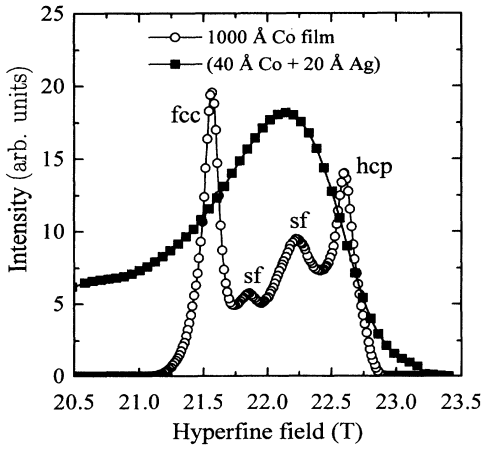


FIG. 1. Comparison of the NMR spectrum of a 1000 Å thick Co film and the bulk part of the NMR spectrum of a 100×(40 Å Co+20 Å Ag) multilayer. The spectrum of the Co film shows clearly separated lines of fcc Co (21.6 T), hcp Co (22.6 T), and Co in stacking faults (sf).

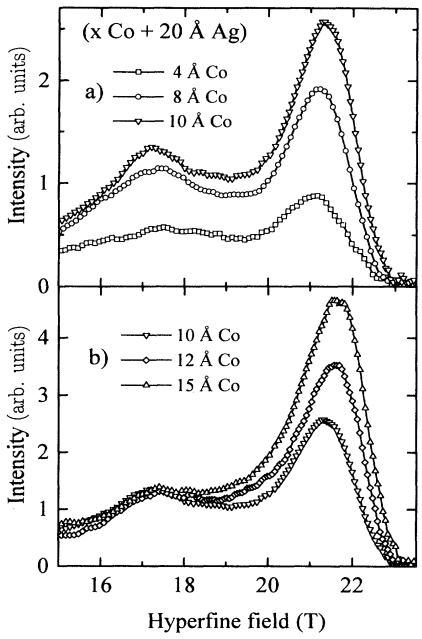


FIG. 2. NMR spectra of the as-deposited ($x$ Å Co+20 Å Ag) multilayers for various nominal Co thicknesses. The integrals (between 15 and 23 T) of the spectra are normalized to the nominal Co thickness. The spectra are corrected for enhancement.

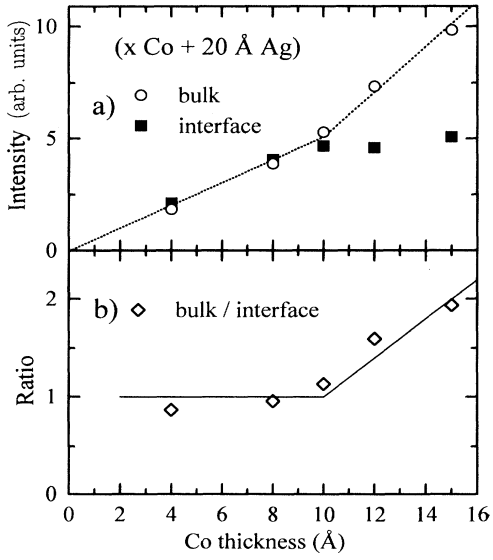


FIG. 3. Intensity of the interface part (a), the bulk part (a), and the ratio between the bulk and the interface part (b), as derived from Fig. 2, as a function of the nominal Co thickness. The dotted line in (a) is a guide to the eye; the solid line in (b) is in accordance with the model discussed in the text.

case of perfect layer-by-layer growth all the Co atoms in the 2-ML-thick Co layers would have Ag neighbors and no bulk Co signal would be present. If the Co layer thickness is increased from 4 to 10 Å both the interface and the bulk intensity increase *proportionally,* as is shown in Fig. 3. This implies that the volume-to-surface ratio of the clusters remains more or less constant. This behavior can only be understood if the growth mode is such that in the nominal Co thickness range 4–10 Å, in first approximation, only the number of three-dimensional islands increases, without appreciable change in shape or size.

Figures 2(b) and 3(a) show that for Co thicknesses increasing from 10 to 15 Å the intensity of the interface signal remains approximately constant, while the number of Co atoms with bulk environment increases. Apparently, for nominal Co thickness $t_{Co} \geq 10$ Å, the additional Co atoms are added to the bulk without changing the number of Co atoms at the interfaces. This observation shows that for Co thicknesses larger than 10 Å (5 ML) the islands mentioned above have merged to form a continuous layer. For nominal thicknesses $t_{Co} \leq 10$ Å, Figs. 2(a) and 3(b) show that the surface-to-volume ratio remains almost constant. A constant value implies, in first approximation, that in this range the Co layers are built with clusters of Co with a thickness of about 5 ML.

Taking these 5 ML for the thickness of the islands and assuming that the islands are laterally rectangular or circular with perfectly flat interfaces, the lateral dimensions of the islands can be estimated by using the experimental fact that the number of Co atoms in the bulk is roughly equal to the number of Co atoms at the interfaces [bulk-to-interface ratio of 1 as shown in Fig. 3(b)]. This estimation results in about 3000 Co atoms per cluster and in typical lateral length scales of the clusters (pancakes) of about 50 Å.

Figure 3(a) shows that the bulk intensity increases from 4 to 10 Å Co with a certain slope. The fact that this line extrapolates approximately to zero corroborates the conclusion drawn above that the Co grows in the three-dimensional island mode for nominal Co thicknesses smaller than 10 Å and not in the layer-by-layer mode. Such a growth with perfectly smooth interfaces would result in all the Co atoms having Ag neighbors if $t_{Co} \leq 2$ ML and bulk Co atoms only for $t_{Co} > 2$ ML. So this growth mode would result in $I_{bulk}/I_{interface} = 0$ for $t_{Co} \leq 2$ ML. Layer-by-layer growth with a certain roughness at the interfaces results in an intersection of $I_{bulk}/I_{interface}$ with the Co thickness axis of more than 2 ML; see Ref. 18.

Using the same (simple) growth model of three-dimensional islands growth for $t_{Co} < 10$ Å and continuous layer growth for $t_{Co} > 10$ Å we can predict the increase of the bulk-to-interface ratio above the nominal thickness of 10 Å, since in our model all additional Co above this thickness contributes to the bulk intensity. The resulting prediction is shown by the solid line in Fig. 3(b) and agrees rather well with the experimental data for the Co thicknesses above 10 Å.

In Fig. 4 a schematic view of the resulting model for the microstructure of the Co/Ag multilayers, as obtained from NMR, is given: discontinuous Co layers for nominal Co thicknesses smaller than about 10 Å and continuous Co layers for Co thicknesses larger than 10 Å. For the sample with a nominal Co thickness of 4 Å about 40% of the area between two Ag layers is covered with Co since the thickness of the Co clusters is about 10 Å. Transmission electron microscopy (TEM) on a similar (6 Å Co+35 Å Ag) multilayer confirmed the discontinuity of the thin Co layers. The TEM pictures showed clumping and columnar growth with discontinuities at the boundaries.[3]

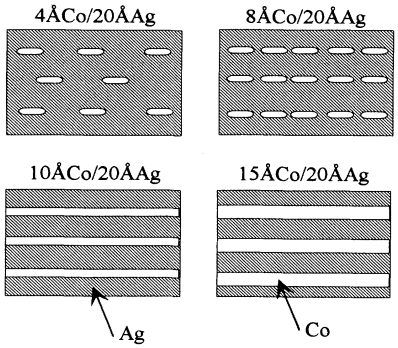


FIG. 4. Schematic presentation of the microstructure of the ($x$ Å Co+20 Å Ag) multilayers with thin Co layers.

### B. Magnetization

In this section we will focus on the magnetic behavior of the Co/Ag multilayers and compare the results with the model of the microstructure of the Co/Ag multilayers proposed above. In Fig. 5 some of the magnetization curves of the series ($x$ Å Co+20 Å Ag), with the applied field both parallel and perpendicular to the film plane, are shown. Obviously, the magnetic anisotropy (the area between the in-plane and perpendicular magnetization curves) decreases steadily with decreasing nominal Co thickness till, for $t_{Co} = 2$ Å, a completely isotropic behavior is observed (also a decrease of the remanent magnetization can be observed, which we will discuss later on). It would be tempting to relate this decrease of the anisotropy straight away to the aforementioned transition from continuous layers to clusters when $t_{Co}$ decreases. One has to recall, however, that such a decrease of the anisotropy is quite common also in multilayers with permanently continuous layers, where it is induced by the interplay of interface anisotropy and shape anisotropy, yielding a critical thickness at which the two contributions balance each other. In fact, from earlier measurements on Co/Ag multilayers[19–21] and from anisotropy determinations on these samples with $t_{Co} > 10$ Å, one may deduce from the usual $Kt_{Co}$ versus $t_{Co}$ plots that such a balancing will occur in the range $t_{Co} \sim 5$ Å, which is in the thickness regime studied here. However, the strong increase of the saturation field for the magnetically isotropic 2 Å Co sample, also apparent from Fig. 5, indicates a behavior different from that observed in continuous layers.[22] In order to discriminate between continuous

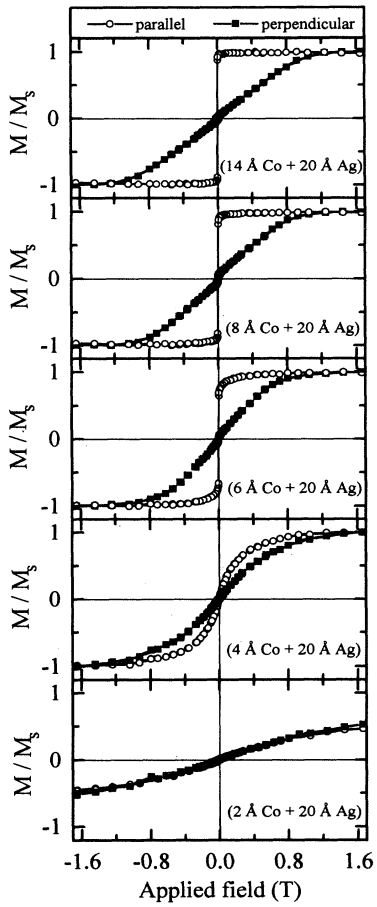


FIG. 5. Field dependence of the magnetization of the $100\times(x$ Å Co+20 Å Ag) multilayers for nominal Co thicknesses between 2 and 14 Å. The measurements were performed at room temperature with the applied field parallel (open circles) and perpendicular (solid squares) to the film plane.

and discontinuous layers the temperature and field dependence of the magnetization of the sample (2 Å Co+20 Å Ag) have been studied.

In Fig. 6 the results of these measurements are displayed. These magnetization curves resemble superparamagnetic behavior as found for various granular systems.[23,24] The magnetization ($M$) can be reasonably described with the Langevin function [$L(\alpha)$]:

$$\frac{M}{M_s}=L(\alpha)=\coth\alpha-\frac{1}{\alpha}\ , \tag{1}$$

with $M_s$ the saturation magnetization and $\alpha=(N\mu_{\mathrm{Co}}H)/(k_BT)$. $N$ is the number of Co spins per cluster, $\mu_{\mathrm{Co}}$ is the magnetic moment per Co atom, $H$ is the applied field, and $T$ is the temperature. Moreover, if we plot the magnetization versus the applied field divided by the temperature ($H/T$) all the curves coincide, as is shown in Fig. 7. Fitting the magnetization curves with the Langevin function yields the number of Co atoms per Co cluster (assuming $\mu_{\mathrm{Co}}=\mu_{\mathrm{Co}}^{\mathrm{bulk}}$). For the sample with a nominal Co thickness of 2 Å this results in about 300 Co

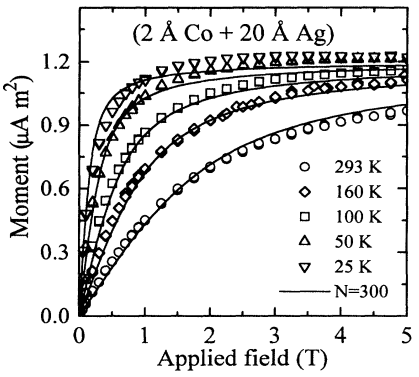


FIG. 6. Field dependence of the magnetization of the sample $100\times(2$ Å Co+20 Å Ag) measured at various temperatures between 25 and 293 K with the applied field parallel to the film plane.

atoms per cluster. The magnetization at various temperatures calculated with Eq. (1) and $N=300$ is represented by the solid lines in Fig. 6. Although this experiment corroborates the granular nature of the system, the number of Co atoms per cluster for the sample with 2 Å Co seems much smaller than the cluster size estimated from the NMR experiments for the samples in the range $4<t_{\mathrm{Co}}<10$ Å (~3000 atoms). Note, however, that the latter estimate was based on the somewhat simplified conclusion that the ratio between the number of bulk and interface atoms equals 1 in the whole range below $t_{\mathrm{Co}}=10$ Å. For the present system with $t_{\mathrm{Co}}=2$ Å this ratio may be smaller [see Fig. 3(b)], which accounts for at least part of the difference.

Another indication for the presence of magnetic clusters is the observation of a blocking temperature ($T_B$) if the magnetic moment is measured as a function of the temperature. In Fig. 8 the field-cooled (FC) and zero-field-cooled (ZFC) behavior of the sample (2 Å Co+20 Å Ag) is plotted. The ZFC and FC curves diverge for tem-

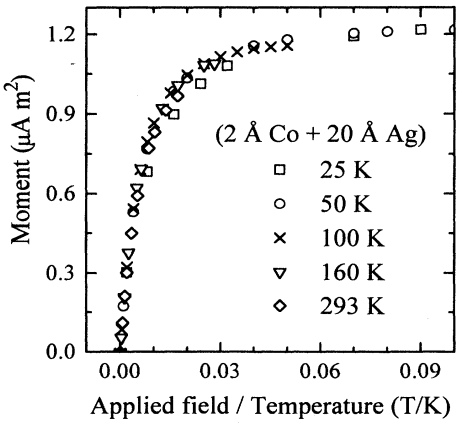


FIG. 7. Magnetic moment as a function of the applied field divided by the temperature for the sample $100\times(2$ Å Co+20 Å Ag).

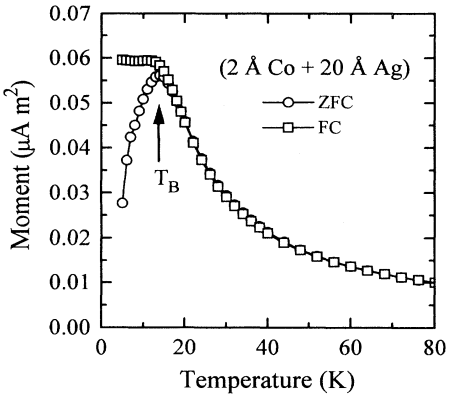


FIG. 8. Field-cooled (FC) and zero-field-cooled (ZFC) magnetization measured in a field of 50 Oe applied parallel to the film plane for the sample 100×(2 Å Co+20 Å Ag). The maximum in the ZFC curve occurs at 15 K.

peratures smaller than about 15 K and the ZFC curve shows a maximum at about 15 K. For larger nominal Co thicknesses $T_B$ increases and the slope of the FC and ZFC curves for temperatures above the blocking temperature changes from paramagnetic ($\sim 1/T$) to ferromagnetic (almost constant). This observation, combined with the increase of the magnetic anisotropy, indicates that for increasing Co thickness a transition occurs from an isotropic granular Langevin-like superparamagnetic system to an anisotropic layered ferromagnetic system.

Besides the decrease of the anisotropy for decreasing $t_{Co}$, the in-plane remanent magnetization ($M_r$) also decreases for decreasing $t_{Co}$, as shown in Fig. 9. In many studies,[25] also for Co/Ag, the value $M_r/M_s$ is interpreted as an indication of the strength of the antiferromagnetic (AF) interlayer coupling (or the fraction of the sample that is coupled antiferromagnetically). AF coupling, however, is not the only mechanism which reduces $M_r$; anisotropy,[22] superparamagnetism, and demagnetization by interparticle magnetostatic interactions can also have this effect. Figure 9 shows that $M_r$ strongly depends on $t_{Co}$ at a constant $t_{Ag}$, which reveals that for this system the deviation of $M_r$ from $M_s$ is not simply related to the AF coupling.

To investigate whether AF coupling of the Co layers over the Ag layers is important in our Co/Ag multilayers, we studied two series with constant Co layer thickness and variable Ag layer thickness. In one series the Co layers were continuous ($t_{Co}=20$ Å); the other series had discontinuous Co layers ($t_{Co}=6$ Å). In Fig. 10 some of the in-plane magnetization curves measured on the series with 6 Å Co are shown. As is shown in the inset, the remanent magnetization shows a monotonic decrease for increasing Ag layer thickness. If the deviation of the remanent magnetization from the saturation magnetization were caused by antiferromagnetic coupling of the Co over the Ag, one would expect the remanent magnetization to *increase* for increasing Ag layer thickness. This is clearly not what Fig. 10 shows. Even for a Ag layer thickness of 60 Å, which is large enough to decouple the Co layers, the remanent magnetization is small. The remanent magnetization of the series with the continuous Co layers ($t_{Co}=20$ Å) was larger than 90% of the saturation magnetization and independent of the Ag layer thickness.

From this we conclude that the small values of the remanent magnetization for the samples with Co layer thicknesses smaller than 10 Å are not caused by antiferromagnetic coupling, but are due to the transition from a layered ferromagnetic system to a granular superparamagneticlike system. The decrease of the remanent magnetization for increasing Ag layer thickness for the series with 6 Å Co is probably the result of better decoupling of the Co clusters for thicker Ag spacer layers. For instance, the influence of Co bridges through the Ag spacer layer (pinholes), which connect the Co clusters and couple the clusters ferromagnetically (higher remanent magnetization), will be smaller for thicker Ag layers.

To summarize, the magnetic behavior of the Co/Ag multilayers with variable Co layer thickness corroborates

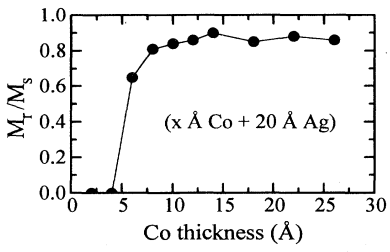


FIG. 9. Remanent in-plane magnetization of the 100×($x$ Å Co+20 Å Ag) multilayers.

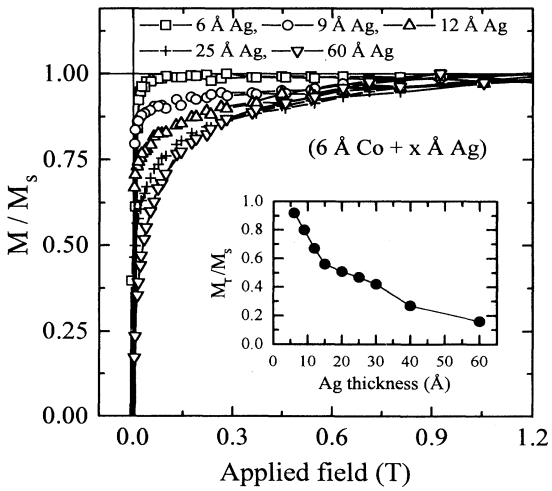


FIG. 10. Field dependence of the magnetization of the 100×(6 Å Co+$x$ Å Ag) multilayers for nominal Ag thicknesses between 6 and 60 Å. The measurements were performed at room temperature with the applied field parallel to the film plane. The inset shows the remanent magnetization as a function of the Ag spacer-layer thickness.

the model of the microstructure of the Co/Ag multilayers proposed on basis of the NMR experiments. Moreover, the magnetization measurements show that the multilayers with very small nominal Co thicknesses show superparamagnetic behavior.

### C. Magnetoresistance

In this section we will try to relate the magnetotransport properties of the Co/Ag multilayers to the microstructural properties and magnetic properties reported above. In Fig. 11 the field dependence of the MR of some samples from the series ($x$ Co+20 Å Ag) with small deposition rates is given. It is clear that the available magnetic fields are not large enough to obtain complete saturation. In this paper the change of the resistance in a field interval of 0 to 1.3 T ($\Delta R$), divided by the resistance at zero field, is used as a definition of the magnitude of the MR.

The shape of the MR curve for the sample with 2 Å Co resembles the behavior of the MR of a granular system. According to Xiao, Jiang, and Chien[26] the MR of such a system can be described with $-A(M/M_s)^2$, where $M$ is the global magnetization and $M_s$ the saturation magnetization. The solid line in Fig. 11 for $t_{Co}=2$ Å is obtained from this equation, with $(M/M_s)$ deduced from the magnetization measurement at 293 K (Fig. 6) and $A$ equal to 0.16. The MR curves for the multilayers with larger nominal Co thicknesses show a sharp drop in resistance at low fields and a large tail at high fields. The MR of these samples is possibly the sum of spin-value MR and a contribution of scattering on magnetic fluctuations (spin-disorder MR).[27]

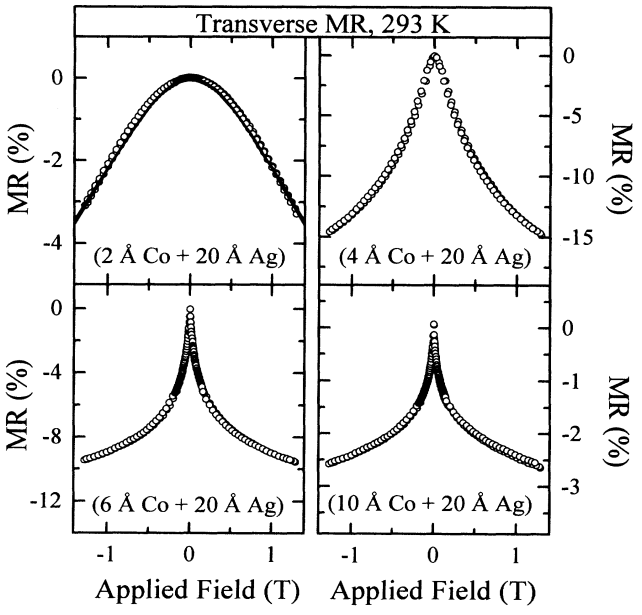


FIG. 11. Field dependence of the magnetoresistance with the applied field parallel to the film plane for ($x$ Co+20 Å Ag) multilayers with nominal Co thicknesses of 2, 4, 6, and 10 Å. The magnetoresistance is defined as $(R_{B=0}-R_{B=1.3\,T})/R_{B=0}$ and was measured at room temperature. Note the differences in the scales of the $y$ axes [magnitude of the MR (%)]. The MR data of the multilayer with 2 Å Co are compared with the function $-A(M/M_s)^2$ with $A=0.16$ (solid line).

The magnitude of the MR as a function of the Co thickness for the series ($x$ Å Co+20 Å Ag) is plotted in Fig. 12 and shows a strong increase of the MR for nominal Co thicknesses smaller than 10 Å. The small MR value of the sample with 2 Å Co *at room temperature* is caused by the fact that this sample shows superparamagnetic behavior and an applied field of 1.3 T at 293 K is not enough to saturate the magnetization, as is shown in Fig. 6. At 10 K the difference of the MR of the sample with 2 Å Co and the sample with 4 Å Co is much smaller. The largest MR value is found for the (4 Å Co+20 Å Ag) multilayer (36% at 10 K for $\Delta R/R_{B=0}$ and 56% at 10 K for $\Delta R/R_{B=1.3\,T}$). In this sample the Co layers are discontinuous and the sample is a mixture of a granular system and a layered ferromagnetic system. The magnitude of the MR is comparable to the values reported by Araki[1] and Loloee *et al.*[3] for similar Co/Ag multilayers.

The increase of the MR for decreasing nominal Co thicknesses, specifically below 10 Å, as is shown in Fig. 12, reflects the transition from continuous ferromagnetic Co layers to a layered granular system that was observed by NMR. Since the size of the Co clusters is approximately constant for Co thicknesses below 10 Å, a further decrease of the nominal Co thickness increases the lateral cluster distances, which leads to further decoupling. The cluster formation and accompanying progressive decoupling of the clusters, also monitored by the reduction of $M_r$ (Fig. 9), yield an array of clusters with a more or less randomly oriented magnetization, which is one of the necessary ingredients for a giant magnetoresistance effect. The decoupling can be promoted by the isolation of pinholes between the layers, as suggested by Hylton *et al.* for the NiFe/Ag system.[8] Earlier reports suggest that, in the case of Co/Ag also, pinholes strongly dominate the

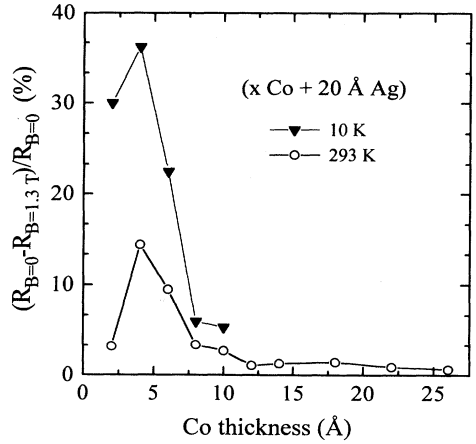


FIG. 12. Magnitude of the magnetoresistance with the applied field parallel to the film plane as a function of the nominal Co thickness for the Co/Ag multilayers with small deposition rate. The measurements were performed at room temperature and at 10 K.

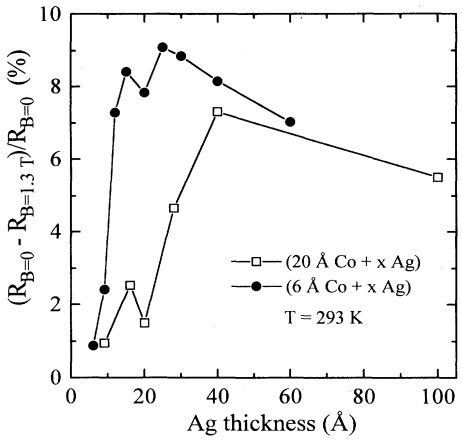


FIG. 13. Magnitude of the magnetoresistance with the applied field parallel to the film plane as a function of the nominal Ag thickness of the two series of Co/Ag multilayers with different Co layer thickness. The measurements were performed at room temperature.

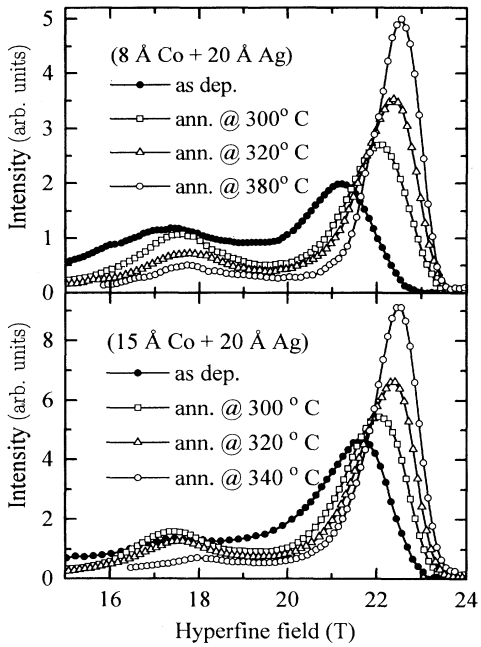


FIG. 14. NMR spectra of (8 Å Co+20 Å Ag) and (15 Å Co+20 Å Ag) multilayers after different annealing treatments. The spectra are normalized to the nominal Co thickness and corrected for enhancement.

interlayer coupling.[28,29] The decrease of $M_r$ in (6 Å Co+$x$ Ag) with increasing Ag thickness, as shown in Fig. 10, strongly supports the view of decoupling by isolation of pinholes through the Ag layer. This effect can also be observed in Fig. 13, where the MR for continuous and discontinuous Co layers as a function of the Ag layer thickness is compared. For the Co/Ag multilayers with continuous Co layers ($t_{Co}=20$ Å) the MR rises from a low value for small Ag layer thicknesses, the regime of ferromagnetic pinhole coupling, to a higher value around 40 Å Ag, where the density of pinholes will be drastically reduced[28,29] and the layers will be decoupled. For the granular-type layers ($t_{Co}=6$ Å) the decoupling occurs at much smaller Ag thicknesses, due to the isolation of the pinholes that are present.

## IV. ANNEALING

### A. Structure

In this section we will present the results of our study of the effects of annealing of the above discussed Co/Ag multilayers on the structural properties (monitored by NMR) and the magnetization, as well as the resulting changes in the MR. The NMR spectra of the (8 Å Co+20 Å Ag) multilayer (discontinuous Co layers) and of (15 Å Co+20 Å Ag) (continuous Co layers) for different annealing temperatures are shown in Fig. 14. Several features are noteworthy and will be briefly discussed in the next paragraphs.

For both systems a systematic increase of the bulk intensity at the expense of the total interface intensity can be observed upon annealing. Simultaneously, the shape of the interface spectrum changes. For both systems the spectrum tends to narrow around 17.5 T. For the 8 Å Co layer this is accompanied by a gradual decrease of the spectral intensity at 17.5 T, whereas for the 15 Å Co layer the decrease occurs abruptly.

To interpret these features one should recall that the interface spectrum consists of contributions of Co atoms with imperfect surroundings together with the spectral line at 17.5 T which represents the contribution of Co at perfectly flat (111) interfaces. The decrease of the interface intensity, except for the line at 17.5 T, and the increase of the bulk intensity at the lower annealing temperatures must be caused by sharpening of the interfaces. Because Co and Ag are immiscible elements, annealing will result in smoothing of the interfaces. For a (111) Co/Ag interface this will result in a relative increase of the number of Co atoms at the interface having three Ag neighbors [flat (111) interfaces] and a decrease in the number of Co atoms with 1, 2, 4, 5, etc. Ag neighbors (imperfect surroundings).

Apart from this sharpening of the interfaces for both systems, the gradual increase of the number of bulk atoms at the expense of the number of the interface atoms for higher annealing temperatures in the 8 Å Co system can only be explained by a transition of the pancakelike clusters, already present in the system, to more spherical-shaped clusters or by growth of the clusters.

For the 15 Å Co+20 Å Ag sample with continuous Co layers this process is markedly different. Increasing the annealing temperature only results in sharpening of the interface, while the surface area (monitored by the intensity of the 17.5 T line) persists until at a critical annealing temperature the surface contribution is drastically reduced. This can only be explained by the transformation of the continuous layers to rather bulky clusters. Such a transition from continuous to discontinuous magnetic

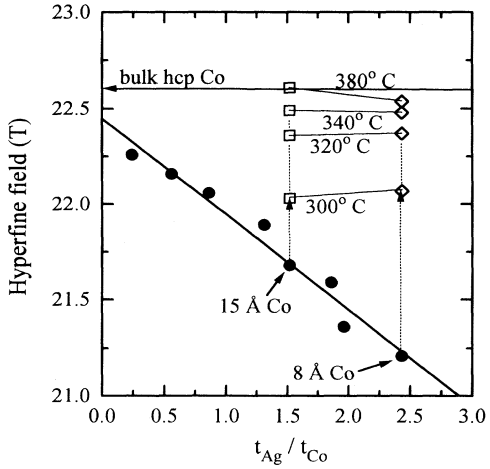


FIG. 15. Position of the main NMR line of the Co/Ag multilayers as a function of the ratio between the Ag thickness and the Co thickness. The solid circles are the positions for the as-deposited samples. The solid line through the data points is a fit with the incoherent model [hyperfine field proportional to $1/t_{Co}$ (Ref. 17)]. The hyperfine fields of the main line after successive annealing of the samples with 8 and 15 Å Co are given by the diamonds and the squares, respectively.

layers upon annealing is also found by Hylton and coworkers[8,30] and Bian *et al.*[9] for NiFe/Ag multilayers.

Apart from this, Fig. 14 shows a clear shift of the position of the main line (bulk Co atoms) of both samples to higher hyperfine fields if the annealing temperature increases. These shifts are attributed to strain effects. In the as-deposited Co/Ag multilayers these effects have been reported in a separate publication.[17] The shift of $B_{hf}$ upon annealing is caused by relaxation of the strain in the Co lattice, which is attributed to the growth of the Co clusters and to the reduction in the degree of coherence between the Co and the Ag lattice upon annealing.[7] In Fig. 15 the relaxation of the strain for the two annealed Co/Ag multilayers is shown in more detail. From this figure it can be seen that the strain is mainly relaxed after the first two annealing treatments (300 and 320 °C). Ultimately the strain is totally relaxed and $B_{hf}$ almost equals the value of bulk hcp Co (22.6 T) which is larger than the value of $B_{hf}$ of the as-deposited Co/Ag multilayers extrapolated to infinitely thick Co layers (22.4 T). This implies that the shift of the hyperfine field upon annealing is caused not only by strain relaxation but also, for a small amount, by a transition to a more hexagonal phase of Co.

### B. Magnetization and magnetoresistance

In the previous section we have seen that annealing of the Co/Ag multilayers with discontinuous Co layers results in a transition of the shape of the Co clusters from flat pancakelike to more spherical and in cluster growth. For the as-deposited continuous Co layers, annealing results in breaking of the Co layers and subsequent cluster formation. In this section we will examine whether the behavior of the magnetization and the magnetoresistance can be related to these structural transitions.

A typical example of the influence of annealing on the magnetization is given in Fig. 16, where the field dependence of the magnetization of the as-deposited (10 Å Co+20 Å Ag) sample and that sample after annealing at 400 °C is plotted. This figure shows the general trends of the changes upon annealing for the Co/Ag multilayers that display characteristic ferromagnetic-layer magnetization loops in the as-deposited state. As is apparent, both the magnetic anisotropy (the area between the in-plane and perpendicular magnetization curve) and the in-plane remanent magnetization decrease upon annealing. For the samples with the discontinuous Co layers ($t_{Co} < 10$ Å) a similar trend was observed, although the as-deposited layers already showed a reduced anisotropy and remanance compared to the Co/Ag multilayers with continuous Co layers (see Fig. 5). As a consequence, the magnetization of the sample with 4 Å Co was almost isotropic after the first annealing treatment at 300 °C. The observation that the annealed samples show a reduced magnetic anisotropy correlates perfectly with the NMR findings: flat pancakelike islands obviously have a larger shape anisotropy than more spherically shaped clusters.

The effect of annealing on the MR was studied in a series ($x$ Å Co+20 Å Ag) with $x$ between 2 and 14 Å. As an example, Fig. 17 shows the influence of annealing on the MR of the sample (8 Å Co+20 Å Ag). Plotted is the MR measured at room temperature with the applied field parallel to the film plane for various anneal temperatures. The maximum MR is found after annealing at 380 °C and is three times as large as the MR of the as-deposited sample. In Fig. 18 the magnitude of the MR as a function of the annealing temperature of this sample and the other samples of this series is shown. The figure clearly demonstrates that the influence of annealing on the magnitude

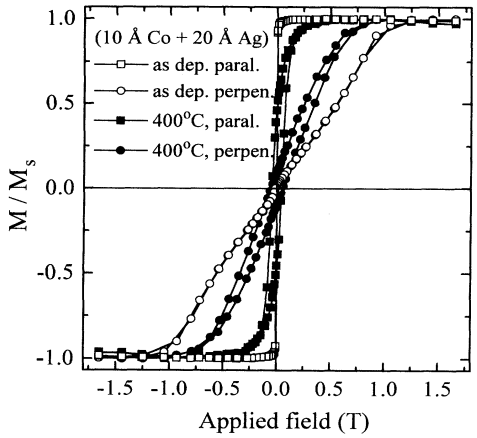


FIG. 16. Influence of annealing on the in-plane (squares) and perpendicular (circles) magnetization of the sample 100×(10 Å Co+20 Å Ag). The as-deposited data are given by the open symbols, whereas the closed symbols represent the data after annealing at 400 °C. The measurements were performed at room temperature.

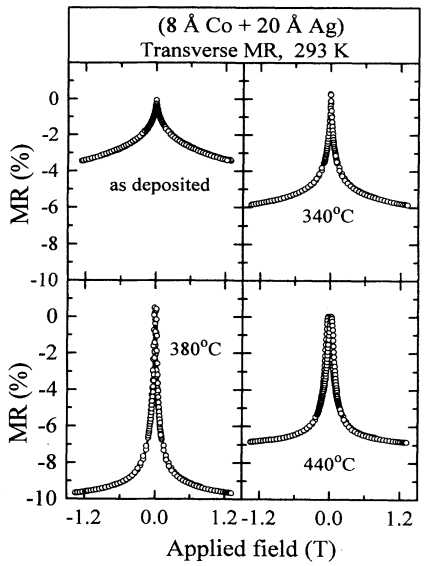


FIG. 17. Influence of annealing on the field dependence of the magnetoresistance of the 100×(8 Å Co+20 Å Ag) multilayer. The magnetoresistance defined as $(R_{B=0}-R_{B=1.3\ T})/R_{B=0}$ was measured at room temperature with the applied field parallel to the film plane.

of the MR strongly depends on the nominal thickness of the Co layer. For the samples with 2, 12, and 14 Å Co the MR is approximately unaffected by annealing treatments, the MR of the sample with 4 Å Co monotonically decreases upon annealing, whereas for the samples with 6, 8, and 10 Å Co the MR shows a maximum at a certain annealing temperature.

A study by Tosin *et al.*[31] of the changes of the MR of (15 Å Co+$x$ Å Ag) multilayers, with $45<x<65$ Å, upon annealing showed a maximum in the MR at about 350 °C. For these electron-beam-deposited multilayers the maximum MR was approximately 5% at room temperature.

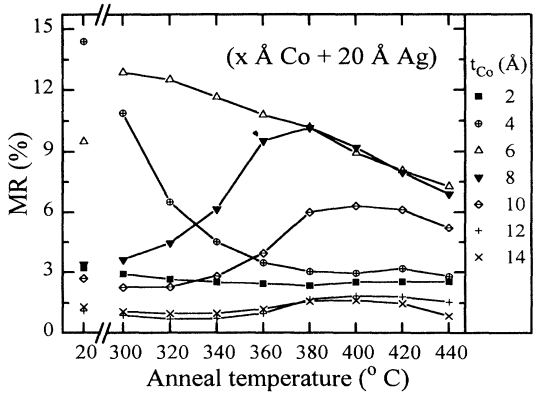


FIG. 18. Magnetoresistance versus annealing temperature for 100×($x$ Å Co+20 Å Ag) multilayers with $2<x<14$ Å. The magnetoresistance was measured at room temperature and is defined as $(R_{B=0}-R_{B=1.3\ T})/R_{B=0}$.

In order to understand the influence of annealing on the MR, we will discuss the changes in the microstructure upon annealing, and the consequences for the MR. For granular Co-Ag systems it has been shown that the cluster size, which depends on the deposition conditions, fraction of Co, and the anneal treatment, is very important for the magnitude of the MR.[7,26,32] In the present case, for Co thicknesses smaller than about 10 Å, the Co layers are discontinuous and consist of pancakelike Co clusters which are partly ferromagnetically coupled. The ferromagnetic coupling of the islands, either directly within the layer or indirectly via interlayer pinholes, depends on the distances between the Co clusters, which in turn depends on the shape and sizes of the Co clusters. Annealing results in a transition of the shape of the clusters from flat pancakelike to more spherically shaped and in growth of the Co clusters. This leads to an increase of the lateral distances of the Co clusters, which results in further decoupling of these clusters and, in principle, in an *increase* of the MR. However, the growth of the Co clusters also results in a decrease of the interface-to-volume ratio, directly monitored by NMR. Because for Co/Ag interface scattering is believed to be very important for the existence of MR,[7,33] the MR depends on the ratio between the mean free path and the cluster size and *decreases* if the Co clusters become too large. The influence of annealing on the magnitude of the MR is determined by the specific microstructure of the Co layers and the net result of above-mentioned effects.

Taking this into consideration, the changes of MR upon annealing for the samples with different nominal Co thicknesses, as shown in Fig. 18, are easy to understand. The MR of the sample with 4 Å Co is already very large in the as-deposited state: the Co clusters are decoupled and have an optimum size for the MR. Annealing results in growth of the Co clusters and an instantaneous decrease of the MR. For samples with a larger initial Co thickness the Co clusters are partly ferromagnetically coupled in the as-deposited state and annealing results in a maximum of the MR at a certain annealing temperature (e.g., 8 Å Co). Annealing of samples with continuous Co layers results in breaking of the layers (as is shown above with NMR) and also in a maximum of the MR upon annealing. Nevertheless, the change of the MR upon annealing is very small because the initial thickness of the magnetic layer is so large that the size of the clusters formed is larger than the optimum determined by the mean free path (e.g., for 14 Å Co). Another explanation for the observation that the changes in the MR upon annealing are small for the samples with relatively thick magnetic layers is the fact that for these samples it might be impossible to decouple the magnetic clusters sufficiently because there is too much Co present.

From the NMR study we have seen that, besides the growth of the Co clusters, annealing also results in smoothing of the interfaces and relaxation of the strain. Because both these processes mainly occur during the first two annealing treatments (see Figs. 14 and 15) and because these processes behave monotonically, they cannot explain the maxima in the magnitude of the MR as a function of the annealing temperature.

## V. CONCLUSIONS

NMR, magnetoresistance, and magnetization studies show that the magnetic behavior of Co/Ag (111) multilayers depends strongly on the nominal thickness of the Co layers, which determines the microstructure of the Co layers. The magnitude of the MR is determined by the following microstructural characteristics of the Co: continuous layers or clusters, size of the clusters, distances between the clusters, and pinholes. Two regimes can be distinguished. For Co thicknesses larger than about 10 Å the Co layers are continuous and a ferromagnetic layered system results. The magnitude of the MR in this regime depends strongly on the thickness of the Ag layer. If this thickness is too small, ferromagnetic bridges of Co through the Ag layers cause ferromagnetic coupling and strongly diminish the MR ratios. For smaller nominal Co thicknesses (2–8 Å) the Co layers are discontinuous and the system can be considered as a layered granular system. Due to the discontinuity of the Co layers the pinholes are isolated, which results in high MR ratios. For very small Co thicknesses (2 Å) the magnetization is isotropic and the Co clusters show superparamagnetic behavior: the magnetization can be reasonably described with the Langevin function and blocking occurs at a temperature of about 15 K.

In a recent study of magnetization, magnetoresistance, and TEM of as-deposited sputtered Co/Ag multilayers in the regime $2 < t_{Co} < 35$ Å and $5 < t_{Ag} < 150$ Å, Loloee *et al.*[3] arrive at similar conclusions about the microstructure of the as-deposited systems. In contrast to the results of Loloee *et al.*[3] and of Araki,[1] neither the magnetization nor the magnetoresistance measurements of the present Co/Ag multilayers showed any indication of antiferromagnetic coupling.

The NMR measurements have shown that the microstructure of the Co layers depends on the nominal Co thickness and the annealing treatment. Since the MR depends strongly on the microstructure, it also depends on the nominal Co thickness and the annealing treatment. The most important changes upon annealing are decoupling of the Co clusters, for the continuous layers after breaking of the layers, and growth of the Co clusters. We have shown that, depending on the initial microstructure of the Co, the MR can initially either increase or decrease upon annealing. Ultimately, at high annealing temperatures, the MR of all the samples decreases upon annealing, due to the growth of the Co clusters.

## ACKNOWLEDGMENTS

The authors gratefully acknowledge the Michigan State University, where two series of the Co/Ag multilayers were produced in the sputtering system funded by the U.S. National Science Foundation, under Grant No. DMR-9122614, and the MSU Center for Fundamental Materials Research. The other Co/Ag multilayers were sputtered at Philips Research Laboratories Eindhoven. The authors would like to thank P. A. A. van der Heijden and A. H. Kamp for experimental assistance and H. J. M. Swagten for stimulating discussions. This research was supported in part by the European Community Science Project ESPRIT3 Basic Research, "Study of Magnetic Multilayers for Magnetoresistive Sensors" (SmMmS).

[1] S. Araki, J. Appl. Phys. **73**, 3910 (1993).

[2] M. Tan, J. A. Barnard, M. R. Parker, and D. Seale, in *Magnetic Ultrathin Films: Multilayers and Surfaces/Interfaces and Characterization,* edited by B. T. Jonker, S. A. Chambers, R. F. C. Farrow, C. Chappert, R. Clarke, W. J. M. de Jonge, T. Egami, P. Grünberg, K. M. Krishnan, E. E. Marinero, C. Rau, and S. Tsunashima, MRS Symposia Proceedings No. 313 (Materials Research Society, Pittsburgh, 1993), p. 191.

[3] R. Loloee, P. A. Schroeder, W. P. Pratt, Jr., J. Bass, and A. Fert, Physica B (to be published).

[4] W. P. Pratt, Jr., S. F. Lee, J. M. Slaughter, R. Loloee, P. A. Schroeder, and J. Bass, Phys. Rev. Lett. **66**, 3060 (1991).

[5] J. A. Barnard, S. Hossain, M. R. Parker, A. Waknis, and M. L. Watson, J. Appl. Phys. **73**, 6372 (1993).

[6] J. Q. Xiao, J. S. Jiang, and C. L. Chien, Phys. Rev. B **46**, 9266 (1992).

[7] A. E. Berkowitz, J. R. Mitchell, M. J. Carey, A. P. Young, D. Rao, A. Starr, S. Zhang, F. E. Spada, F. T. Parker, A. Hutten, and G. Thomas, J. Appl. Phys. **73**, 5320 (1993).

[8] T. L. Hylton, K. R. Coffey, M. A. Parker, and J. K. Howard, Science **261**, 1021 (1993).

[9] X. Bian, A. Zaluska, Z. Altounian, J. O. Ström-Olsen, Y. Huai, and R. W. Cochrane, in *Magnetic Ultrathin Films: Multilayers and Surfaces/Interfaces and Characterization* (Ref. 2), p. 405.

[10] X. Bian, Z. Altounian, J. O. Ström-Olsen, A. Zaluska, Y. Huai, and R. W. Cochrane, J. Appl. Phys. **75**, 6560 (1994).

[11] B. Rodmacq, G. Palumbo, and Ph. Gerard, J. Magn. Magn. Mater. **118**, L11 (1993).

[12] T. L. Hylton, K. R. Coffey, M. A. Parker, and J. K. Howard, J. Appl. Phys. **75**, 7058 (1994).

[13] T. L. Hylton, Appl. Phys. Lett. **62**, 2431 (1993).

[14] E. A. M. van Alphen, H. A. M. de Gronckel, P. J. H. Bloemen, A. S. van Steenbergen, and W. J. M. de Jonge, J. Magn. Magn. Mater. **121**, 77 (1993).

[15] H. A. M. de Gronckel, P. J. H. Bloemen, E. A. M. van Alphen, and W. J. M. de Jonge, Phys. Rev. B **49**, 11 327 (1994).

[16] K. Sakai and T. Kingetsu, J. Cryst. Growth **126**, 184 (1993).

[17] E. A. M. van Alphen, S. G. E. te Velthuis, H. A. M. de Gronckel, K. Kopinga, and W. J. M. de Jonge, Phys. Rev. B **49**, 17 336 (1994).

[18] H. A. M. de Gronckel and W. J. M. de Jonge, in *Magnetism and Structures in Systems of Reduced Dimension,* edited by R. F. C. Farrow *et al.* (Plenum, New York, 1993).

[19] F. J. A. den Broeder, W. Hoving, and P. J. H. Bloemen, J. Magn. Magn. Mater. **93**, 562 (1991).

[20] R. Krishnan, M. Porte, and M. Tessier, J. Magn. Magn. Mater. **103**, 47 (1992).

[21] T. Kingetsu and K. Sakai, J. Appl. Phys. **73**, 7622 (1993).

[22] P. J. H. Bloemen and W. J. M. de Jonge, J. Magn. Magn. Mater. **116**, L1 (1992).

[23] J. A. Barnard, A. Waknis, M. Tan, E. Haftek, M. R. Parker,

and M. L. Watson, J. Magn. Magn. Mater. **114**, L230 (1992).
[24]H. Wan, A. Tsoukatos, G. C. Hadjipanayis, Z. G. Li, and J. Liu, Phys. Rev. B **49**, 1524 (1994).
[25]S. Araki and Y. Narumiya, J. Magn. Magn. Mater. **126**, 521 (1993).
[26]J. Q. Xiao, J. S. Jiang, and C. L. Chien, Phys. Rev. Lett. **68**, 3749 (1992).
[27]B. Dieny, S. R. Teixeira, B. Rodmacq, C. Cowache, S. Auffret, O. Redon, and J. Pierre, J. Magn. Magn. Mater. **130**, 197 (1994).
[28]D. H. Mosca, A. Barthelemy, F. Petroff, A. Fert, P. A. Schroeder, W. P. Pratt, Jr., and R. Loloee, J. Magn. Magn. Mater. **93**, 480 (1991).
[29]B. Dieny, V. S. Speriosu, S. Metin, S. S. P. Parkin, B. A. Gurney, P. Baumgart, and D. R. Wilhoit, J. Appl. Phys. **69**, 4774 (1991).
[30]M. A. Parker, T. L. Hylton, K. R. Coffey, and J. K. Howard, J. Appl. Phys. **75**, 6382 (1994).
[31]G. Tosin, L. F. Schelp, M. Carara, J. E. Schmidt, A. A. Gomes, and M. N. Baibich, J. Magn. Magn. Mater. **121**, 399 (1993).
[32]S. Zhang, Appl. Phys. Lett. **61**, 1855 (1992).
[33]W. P. Pratt, Jr., S. F. Lee, Q. Yang, P. Holody, R. Loloee, P. A. Schroeder, and J. Bass, J. Appl. Phys. **73**, 5326 (1993).